Accepted Manuscript

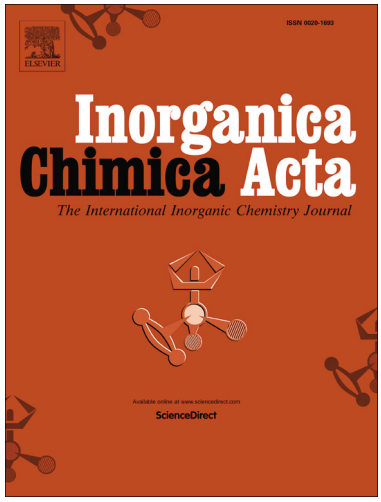

Research paper

Photophysical Properties of Near-IR Cyanine Dyes and their Application as Photosensitizers in Dye Sensitized Solar Cells

William Ghann, Hyeonggon Kang, Edward Emerson, Jiyoung Oh, Tulio Chavez-Gil, Fred Nesbitt, Richard Williams, Jamal Uddin

PII: S0020-1693(17)30443-7
DOI: http://dx.doi.org/10.1016/j.ica.2017.08.001
Reference: ICA 17795

To appear in: *Inorganica Chimica Acta*

Received Date: 22 March 2017
Revised Date: 31 July 2017
Accepted Date: 1 August 2017

Please cite this article as: W. Ghann, H. Kang, E. Emerson, J. Oh, T. Chavez-Gil, F. Nesbitt, R. Williams, J. Uddin, Photophysical Properties of Near-IR Cyanine Dyes and their Application as Photosensitizers in Dye Sensitized Solar Cells, *Inorganica Chimica Acta* (2017), doi: http://dx.doi.org/10.1016/j.ica.2017.08.001

Photophysical Properties of Near-IR Cyanine Dyes and their Application as Photosensitizers in Dye Sensitized Solar Cells

William Ghann[1], Hyeonggon Kang[1], Edward Emerson[1], Jiyoung Oh[1], Tulio Chavez-Gil[1], Fred Nesbitt[1], Richard Williams[2] & Jamal Uddin*[1]

[1] Center for Nanotechnology, Department of Natural Sciences, Coppin State University, 2500 W. North Ave., Baltimore, MD21216

[2]Department of Chemistry, Morgan State University, 1700 E. Cold Spring Ln. Baltimore, MD 21251

*Correspondence and requests for materials should be addressed to J.U. (email: juddin@coppin.edu)

ABSTRACT

The photophysical properties of eight structurally diverse near-infrared cyanine dyes were investigated with respect to their structural features and potential use as light-harvesting sensitizers of dye sensitized solar cells. The absorption, emission, and lifetime characteristics of the dyes were assessed under a variety of condition. The photophysical properties and sensitizing efficiency of three of the eight dyes, with an additional six-membered cyclic ring, were markedly different from the other five. The dyes absorbed light of wavelength within the range of 779 - 823 nm and emitted within the range of 832 – 876 nm. The surface morphology and elemental analysis of the cyanine dye sensitized photoanodes were characterized via Field-Emission Scanning Microscopy Imaging (FESEM) and Transmission electron microscopy (TEM). The current-voltage characteristics and the electrochemical impedance spectroscopic studies were also carried out to calculate solar cell efficiency. The dyes had fluorescence quantum yield

in the range of 14 – 22%. The solar-to- electric power conversion efficiency ranged from 0.04 % to 0.24 %

Key words: NIR, Cyanine dyes, UV-VIS, Emission, Lifetime Decay, IR, FESEM, TEM, I-V and Impedance, DFT calculation

1. Introduction

Dye sensitized solar cells (DSSCs) are a class of photovoltaic devices that have been widely studied due to their advantages, such as ease of fabrication, low cost, and appreciable solar-to-electric energy conversion efficiency [1-7]. DSSCs convert sunlight to electricity using dye molecules which absorb photons and generate electrons [6, 8-10]. Many dye molecules, especially ruthenium polypyridyl complexes, have been used in the fabrication of DSSC, but their wavelength region is only in the UV-Visible range [11-13]. Others have used the co-sensitization of dyes to reduce energy gap sand cover wider regions of the electromagnetic radiation, but the method is quite burdensome [14-18]. Cyanine dyes are a group of dyes that are not frequently explored for use in DSSC due to their relatively long absorption/emission wavelengths [19-20]. They are fluorescent organic dyes made up of two nitrogen-containing heterocycles joined together by a polymethine chain [21-28]. They have been used in various biomedical applications as sensors and imaging agents and have specifically been used for real time detection of cellular function or malfunction [23-25].

Cyanine dyes have shown promise as excellent photosensitizers for DSSC [4, 31-33]. It has been shown that upon adsorption of cyanine dyes to TiO_2 film, the absorption band of the cyanine

dye broadens to the red and blue regions in comparison with their absorption spectra of the dyes in plain solvent. A larger absorption intensity and a broader absorption spectra insure a greater light to electricity conversion efficiency, which clearly establish the proof of principle of fluorescence redox-switching for cyanine derivatives, with more intense fluorescence in the "on" state that is certainly desirable for any practical use compared to other systems developed so far [10].

Heptamethine cyanine dyes, in particular, are promising additions to DSSC technology due to their high molar absorption coefficient in the near infrared (near-IR) region. Heptamethine cyanine dyes are dinitrogen heterocycles linked together by seven methine bridges. In this study, eight heptamethine cyanine dyes, displayed in Figure 1, have been synthesized, characterized and tested for potential DSSC applications. The heptacyanine chromophores, structure were derived from reactions between 2, 3, 3-trimethylindolenine and eight different alkyl halides. Three of the eight heptamethine products are formed by six-membered cyclic ring, attached to a particular polymethine chain. The alkyl groups for the first five heptamethine cyanine derivatives are without the additional six-membered ring are: methyl (Cy1), Ethyl (Cy2), Propyl (Cy3), 2-hydroxy-ethyl (Cy4), and 4-carboxy-butyl (Cy5) Iodide. The remaining three bi-phenyl alkyl three cyanine derivatives are P-methyl (Cy6), P-ethyl (Cy7), and P-butyl (Cy8) iodide, with P=phenyl, respectively.

This study focuses on the photophysical properties of absorption, emission and fluorescence lifetime measurements for the eight structurally diverse near-IR heptamethinecyanine dyes and their potential as photosensitizers in the fabrication of DSSCs. The photophysical properties of

the cyanine dyes were compared by structure and their influence on the efficiency of DSSCs. The photophysical properties of these near-IR cyanine dyes are summarized in Table 1.

2. Experimental Section

2.1 Materials

Titanium dioxide powder (Degussa P25) was purchased from the institute of chemical education. Fluorine tin oxide (FTO) conducting glass slides were purchased from Harford glass company, Hartford City, Indiana. Sodium Hydroxide (NaOH), acetone (C_3H_6O), ethanol (C_2H_5OH), and acetic acid (CH_3COOH) were purchased from Sigma-Aldrich and were used without further purification. Graphite used in making cathode slides was purchased from TED PELLA, INC.

The photoanode was prepared using a fluorine-doped SnO_2 (FTO) conducting glass substrate. The FTO glass slides were cleaned by first washing them a detergent solution and rinsing them with water and ethanol. The FTO glass substrates were subsequently spin coated with TiO_2 paste prepared from TiO_2 powder, acetic acid, and soap water. The TiO_2 coated FTO slides were then annealed at 450 °C for an hour. Using Scanning Electron Microscopy cross-section imaging, the thickness of the TiO_2 layer was found to be approximately 9 µm. To prepare the cathode, graphite paint was spread uniformly on the cleaned FTO glass and allowed to dry in room temperature.

2.2 Synthesis of Cyanine Dyes

The near infrared cyanine dyes were prepared via a microwave assisted organic synthesis. The protocol for the synthesis has been discussed elsewhere [19, 20, 22]. The protocol was optimized using the Biotage single-mode microwave system. For each of the cyanine dyes, one equivalence of N-((E)-(2-chloro-3-((E)-(phenylimino)methyl)cyclohex-2-enylidene)methyl)aniline was made to react with 2 equivalence of the corresponding2,3,3-trimethyl-1-R-3H-indolium iodide in the presence of sodium acetate and ethanol for 20 min at 120°C. Upon completion of each reaction, the reaction vial was cooled to 0°C, filtered, and washed with diethyl ether to obtain greenish-gold crystals with an average yield of 79%. The purified products were characterized using ^{1}H and ^{13}C NMR [19, 20].

2.3 Fluorescence Lifetime Measurements

Cyanine dyes were dissolved in 3 mL of ethanol for fluorescence lifetime solution. To prevent inner filter effect, absorption measurements were carried out to ensure the absorbance of the dyes was less or equal to 0.15 absorbance unit. Fluorescence decays were measured using Horiba Delta-flex fluorescence lifetime system using the time-correlated single-photon counting (TCSPC) technique with the PPD-850 picosecond photon detection module. The excitation source was 785 nm light-emitting diodes (Delta LED) with 785 nm.

2.4 Fabrication of Solar Cell

The photoanode was prepared by depositing a thin film of TiO_2 on the conductive side of fluorine doped tin oxide (FTO) glass using a spin coater and sintered at 380°C for 2 hours [34-

36]. The TiO_2 covered FTO glass was then immersed in a freshly prepared 5mM cyanine dye solution for a period of two hours. The counter electrode (cathode) was prepared by painting FTO glass with colloidal graphite. The cyanine dye-sensitized glass (anode) and the carbon electrode (cathode) were assembled to form a solar cell sandwiched with a redox (I^-/I^{3-}) electrolyte solution.

2.5 Characterization Techniques

Steady-state absorption spectra of cyanine dyes in solution were acquired using UV-3600 Plus from Shimadzu. Steady-state fluorescence spectra were recorded on the fluorescence Nanolog Spectrofluorometer System from Horiba Scientific (FL3-22 iHR, Nanolog). ATR spectra were obtained with a Thermo Nicolet iS50 FTIR. The morphology of each film was analyzed using field emission scanning electron microscopy (FESEM; JSM-7100FA JEOL USA, Inc.). Transmission Electron Microscopy (TEM) images were acquired on JEM-1400 Plus (JEOL USA, Peabody, Massachusetts). The images were viewed using Digital Micrograph software from Gatan (Gatan, Inc, Pleasanton, CA). HOMO and LUMO calculations were carried out using Spartan'14 software from Wavefunction, Inc. Irvine, CA, USA. TiO_2 paste was printed on FTO glass using WS-650 Series Spin Processor from Laurell Technologies Corporation.

2.6 Photovoltaic Properties Measurement

The energy efficiencies of the fabricated cyanine DSSCs were measured using 150 W fully reflective solar simulator with a standard illumination with air-mass 1.5 global filter (AM 1.5 G) having an irradiance corresponding to 1 sun (100 mW/cm^2) purchased from Sciencetech Inc.,

London, Ontario, Canada and Reference 600 Potentiostat/Galvanostat/ZRA from Gamry Instruments (734 Louis Drive, Warminster, PA 18974). The tested solar cells were masked to an area of 5 cm^2. Each cell performance value was taken as the average of three independent samples. The solar energy to electricity conversion efficiency (η) was calculated based on the equation, $\eta = FF \times I_{sc} \times V_{oc}$, where FF is the fill factor, I_{sc} is the short-circuit photocurrent density (mA cm^{-2}), and V_{oc} is the open-circuit voltage (V) as listed in Table 3.

3. Results and Discussion

The photophysical properties of the eight near-IR cyanine dyes were studied to assess their usefulness as sensitizers for dye sensitized solar cells. Absorption and emission spectra measurements, stoke shift calculation, quantum yield, molar absorptivity, and detection sensitivity were determined and are summarized in Table 1. The properties of Cy1-Cy5 were markedly different from the Cy6 to Cy8 which had the additional phenyl group.

3.1 UV-Vis Absorption Studies

The optical properties of the cyanine dyes were investigated using UV-vis spectrometry and the results exhibited in Figure 2. The overall performance of a DSSC depends on the light absorption capability of the dye sensitizer. The absorption characteristics of Cy1 to Cy5 were different from the absorption characteristics of Cy6 to Cy8 which occurred at longer wavelength. The light absorption bands shifted to longer wavelength by 40 nm with the increase in the length of conjugated chain. The absorption peaks of cyanine dyes are known to shift to the red with increasing lengths of the conjugated methine chain [10]. The attachment of the additional six-membered ring increases the photostability of the near-IR cyanine dyes. The rich pi electron

conjugated region of the heptamethine cyanines increases stability in a way that translates into stronger absorption at longer wavelengths. Near-IR absorption and large molar absorptivities are two desired features of sensitizer dyes in DSSC systems. The wavelength of maximum absorption for Cy1 to Cy5 was around 785 nm whereas the wavelength of maximum absorption for Cy6 toCy8 was in the range of 818 - 823 nm. Both of these absorption wavelength regions are desirable as good wavelengths for DSSC sensitizers as well as the accompanying large molar absorption coefficients.

3.2 Steady State Fluorescence Studies

Fluorescence spectra of the cyanine dyes utilized in the fabrication of the DSSC were obtained in order to examine the emission characteristics of the eight dyes. The measurements were carried out with an exciting light (λexc) of 700 nm. The emission pattern of the first five cyanine dyes (Cy1- Cy5) was slightly different from that of Cy6 to Cy8 as shown in Figure 3. While the wavelengths of maximum emission for Cy1 - Cy5 were within the region of 840 nm -843 nm, the wavelength of maximum emission for Cy6 -Cy8 was in the range of 869 – 876 nm. The Stokes shifts at the longer wavelengths are interesting to note. This and the modestly low quantum yields of these dyes, as presented in Table 1, suggest a substantial degree of self-quenching, which competes with the excitation energy needed for electron capture at the anode. Self-quenching occurs when these dyes aggregate. These dyes are known to aggregate, an undesired property for sensitizers, even at low concentrations. However, the aggregation can be minimized by the addition of the addition of long alkyl chains and /or polar constituents such as carboxylic, phosphate, sulfonate, and or hydroxyl groups to the substituent regions or the indolenic nitrogen atoms of the cyanine moles [33, 37]. These substituent groups, in particular,

the carboxylic and hydroxyl groups, also efficiently serve as anchors to the semiconductor electrode (i.e. TiO_2) surface [37].

Self-quenching and the broad absorption spectra of these dyes along suggest favorable Forster Resonance Energy Transfer (FRET) interactions (provided stacking from dye aggregation can be minimized), which can occur with highly energetic luminescent compounds and be used to transfer additional energy to these dyes when they are used as sensitizers [38, 39].

3.3 Fluorescence Lifetime Studies

Fluorescence lifetime (FLT) measurements were carried out to evaluate the length of time the molecules stay in the excited state and how lifetime impacts various parameters associated with dye sensitized solar cells constructed with them. The structural relationship of cyanine dyes to their fluorescence lifetimes has been studied by some number researchers [14]. A scattering solution, ludox, was used to measure the instrument response time (IRF) before the lifetime measurement of the samples. The FLT properties of the dyes are summarized in Table 2. With concentrated solutions, the photoluminescence decay show fast and a slower component of lifetime of the near-IR cyanine dyes in ethanol solution. The two lifetimes suggest the presence of two species in the solution. The shorter lifetime is associated with self-quenching aggregation or coplanar “stacking”, while the longer lifetime is associated with “free” dye [14]. However, with very dilute solution, a single exponential decay is observed as shown in Figure in Figure 4 and Table 1. Four spectra, Cy4 representing the first five different structures (Cy1- Cy5) and Cy6 - Cy8 are displayed in Figure4. In general, the indolenic structure of Cy1 - Cy5 had a longer lifetime (0.18 ns - 0.68 ns) than the benzoindolenic structure of Cy6 –

Cy8 (0.32 ns – 0.43 ns). The short lifetimes of these near-IR dyes pose a potential problem because of the implied competition with electron injection half times. Longer fluorescence lifetimes and shorter electron injection half times are requirements for efficient DSSC's, especially in terms of long term stability a requirement for commercially successful solar cells [40]. In addition to minimizing aggregation, the relationship between dye synthesizers lifetime and electron injection halftimes must be optimized for the effective incorporation of near-IR dyes in DSSC's.

3.4 Field Emission Scanning Electron Microscopy Imaging

The morphological characteristics of the TiO_2 electrode were further investigated using Field-Emission Scanning Microscopy Imaging (FESEM), Energy dispersive X-ray spectroscopic (EDS), and line profile map analysis. Cy5 was used for the SEM and EDS imaging studies because of its carboxylate anchoring groups which interacts well with TiO_2 film. The carboxylate groups present in Cy5 enhance the adsorption of the dye to the titanium dioxide semiconductor surface providing an efficient coupling for the ultrafast injection of electrons [35-38]. Figure 5 shows the FESEM microscopic morphology of the FTO slide with nanocrystalline mesoporous TiO_2 film and a layer of cyanine attached to the surface. No significant change in the surface morphology of the samples was observed before and after dye application. Energy dispersive X-ray spectroscopic (EDS) was also used for the chemical characterization of the cyanine dye sensitized TiO_2/FTO glass (Figure 5b) in comparison with the bare TiO_2 coated FTO glass (Figure 5a). An intense peak for carbon in the dye-sensitized sample as compared to that of the blank was observed. Cyanine dye contains a high percentage of carbon by virtue of the fact that it is

an organic compound. EDS mapping analysis of the cyanine dye sensitized TiO_2/FTO slide (Figure 5 c & d) shows presence of carbon indicative of the presence of organic compound and also Titanium which is suggestive of the presence of TiO_2. It is seen from the line profile image (Figure 5 c &d) that the portion of TiO_2 substrate covered with dye show huge peaks of carbon (red) whereas the portion without dye mostly had only Titanium (green).

3.5 Transmission Emission Microscopy Imaging

To confirm the adsorption of the cyanine dyes on the TiO_2 nanoparticles, the high-resolution images were taken by transmission electron microscopy (TEM, JEM-1400, JEOL Co.) as shown in Figure 6. To get the TEM images, after cyanine dye was dissolved in the ethyl alcohol, the TiO_2 powder was added to the solution. The mixture was suspended for 20 min for the adsorption of the TiO_2 powder and the dye. After then, one drop of the dye mixture was dried on TEM grid in a hood overnight. In addition, as a control, a mixture of TiO_2 and ethyl alcohol was also dried on another TEM grid. Anatase TiO_2 nanoparticles are observed with a particle size range of 20 -25 nm as shown in Figure 6. Rutile TiO_2 nanoparticles are also rarely observed (Figure 6(c)). Small spherical dyes of 1 - 3 nm decorated on the anatase TiO_2 nanoparticles are observed (Figure 6(a) and (b), the arrows in the images guide to the dyes), while any dye shapes are absent in the control as shown in the Figure 6 (c) and (d). It is speculated that the adsorption between the TiO_2 nanoparticles and the dyes results from the electrostatic binding because the dyes do not have any functional groups which are able to induce any binding between them.

3.6 IR Spectroscopy Analysis

The IR spectra of the films annealed at room temperature shows three vibrational modes which are ascribed to TiO_2 [39-41]. The IR measurements, as displayed in Figure 7, were carried out on Cy4 and Cy6 basing of the fact that the behavior of the first five cyanine dyes (Cy1 – Cy5) are slightly different from that of the last three dyes (Cy6 – Cy8). However, the differences between the IR spectra of the two dye-sensitized TiO_2 photoanodes were not significant. An interesting observation in these studies was that the stretching intensities were increased with the deposition of cyanine dyes, with a significant change on the TiO_2 IR modes, which indicates that there occurred an interaction that shifts to low energies the initially TiO_2 stretching. This observation shows that the deposition of cyanine dye undergoes strong phase transition due to an electronic environment change around the TiO_2 energies [32, 36, 37].

3.7 Current-Voltage Characteristics

The I-V characteristics curves of the all eight fabricated cyanine dye sensitized solar cell were measured and analyzed as exhibited in Figure 8. The parameters related to the cell performance such as the short circuit current, open circuit voltage, and fill factor are displayed in Table 3. The I-V measurements were conducted under illumination of 100 mW/cm^2. The highest short circuit current density was obtained for the cell sensitized with Cy1. The higher efficiencies observed in Cy1 to Cy5 may be due to the higher percentage of electron donating groups compared to Cy6 to Cy8 as has been previously established for other cyanine molecules [38].

3.8 Electrochemical Impedance Spectroscopy

The electrochemical impedance spectroscopy (EIS) of the fabricated cells was investigated. EIS is a valuable technique for studying the kinetics and energetics of charge transport and recombination in dye sensitized solar cells [44]. Impedance measurements were carried out at frequencies between 0 and 100 KHz. Figure 9 shows the Nyquist plots and Figure 10, the Bode plot of all the eight cyanine dye employed in the study. Cy2 (30Ω) and Cy3 (55Ω) have the least resistance to current according to the Nyquist plot. Cy6 (130Ω) and Cy8 (110 Ω) had higher resistance. The cyanine dyes with similar structures therefore have similar resistance. The two phenyl groups in Cy6 to Cy8 increase the resistance to flow of current. Cy5 is however an outliner shows the greatest resistance among all the dyes. This is also consistent to the IV data that show Cy5 as having lower efficiency compared to all of the other cyanine dyes with similar structures. Figure 10 shows the Bode phase plot for the cyanine dye sensitized solar cells. Cy2 and Cy3 show a relatively small capacitance compared to that of the other cyanine dyes. The transfer resistance of Cy6 and Cy8 are far higher than that of the other cyanine dyes with the exception of Cy5.

3.9 Density Functional Calculations for Cy5

Density functional calculations were used to optimize the geometry of Cy5 molecule using the software Spartan 16 from Wavefunction. All geometries were computed using the ΩB97X-D density functional theory method. The geometry optimization was performed using 6-31G* basis set. This model was used to calculate the highest occupied molecular orbital (HOMO) and the lowest unoccupied molecular orbital (LUMO) energies of Cy5. The calculations gave a result for the HOMO of -8.86 eV and the result for the LUMO of -3.95 eV . The difference in the HOMO

and LUMO, the band gap, is 4.91 eV. Figure 11 (a & b) shows the Lewis and 3D structures of Cy5. The HOMO and LUMO surfaces and orbital energy diagrams are shown in Figure 12 (a) and Figure 12 (c), respectively. In Figure 12(a) and Figure 12(c) the blue and red regions represent positive and negative values of the orbitals, respectively.

When exposed to radiant energy, dye molecules (S) adsorbed on the TiO_2 film absorb photons and make a transition from the ground state or the highest occupied molecular orbital (HOMO) to an excited state or the lowest unoccupied molecular orbital (LUMO) state as displayed in Figure 12. The photoexcited dye species (S*) injects an electron into the conduction band of TiO_2 electrode and becomes oxidized (S^+). The oxidized dye species subsequently accept an electron from the electrolyte (I^-), and then the ground state of the dye (S) is restored. The injected electron is transported through the mesoporous TiO_2 film to the FTO layer and is conducted through an external circuit to a load where the work done is delivered as electrical energy. The electron from the external load diffuses to the cathode where it gets transferred to the electrolyte (I_3^-), so the electrolyte system is regenerated.

4. Conclusion

In this paper the photophysical properties of synthesized cyanine dyes were evaluated for application as sensitizers for dye sensitized solar cells. Preparation and characterization of cyanine dye sensitized solar cells are presented in this work. The devices were characterized

using absorption spectroscopy, Fluorescence spectroscopy, Field Emission Scanning Electron Microscopy, and Transmission Electron Microscopy. The absorption spectra, electrochemical, and photovoltaic properties were accordingly investigated. The performance characteristics of the devices in terms of current and voltage measurements and Impedance measurement show that near-IR heptamethine cyanines are promising sensitizer dye candidates for DSSC. Overall, Cy1 - Cy5 were found to possess photophysical properties that were different from that of Cy6 to Cy8. In general, the indolenic cyanine dyes (Cy1 – Cy5) showed better photovoltaic performance than the benzo indolenic dyes (Cy6 – Cy8). In all, a short-circuit photocurrent density (I*sc*) in the range of 0.55 – 2.69 $mAcm^{-2}$, an open-circuit photovoltage (V*oc*) of 170 - 390 mV, fill factor of 0.24–0.39, and corresponding conversion efficiency in the range of 0.04- 0.24 % was obtained under the simulated AM 1.5G solar light condition with irradiation of 100 mW/cm^2. The relatively low efficiencies can be linked to the short lifetimes exhibited by the dyes. When the excitation lifetimes of the sensitizers approach the half-life times of electron injection, competition between the two processes becomes more relevant, and lower efficiencies result. The lower efficiencies can also be linked to the absence of anchoring groups on the dyes. The anchoring groups aid the adsorption of the dye to semiconductor TiO_2 which facilitates the injection of electrons.

Acknowledgement

The work was financially supported by the University of Maryland System Wilson E. Elkins Professorship (2485897), Constellation, an Exelon Company, E2- Energy to Educate grant program (163893), and Dept. of Education, SAFRA Title III Grant (2486005). The authors are also grateful to the Institution of Advancement, Coppin State University, for administrative help. The content is exclusively the responsibility of the authors and does not necessarily represent the official views of the funding agencies.

5. References

[1] B. O'Regan, M. Gratzel, A low-cost, high-efficiency solar cell based on dye-sensitized colloidal TiO_2 films. *Nature* 353 (1991) 737-740.

[2] S. Mathew *et al.*, Dye-sensitized solar cells with 13% efficiency achieved through the molecular engineering of porphyrin sensitizers. *Nat. Chem.* 6 (2014) 242-247.

[3] G. K. Singh, Solar power generation by PV (photovoltaic) technology: A review. *Energy* 53 (2013) 1-13.

[4] M. Ye *et al.*, Recent advances in dye-sensitized solar cells: from photoanodes, sensitizers and electrolytes to counter electrodes. *Mater. Today* 18 (2015) 155-162.

[5] H. Hug, M. Bader, P. Mair, T. Glatzel, Biophotovoltaics: Natural pigments in dye-sensitized solar cells. *Appl. Energy* 115 (2014) 216-225.

[6] N. A. Ludin *et al.*, Review on the development of natural dye photosensitizer for dye-sensitized solar cells. *Renew Sust Energ Rev* 31 (2014) 386-396.

[7] W. Ghann et al. Fabrication, Optimization and Characterization of Natural Dye Sensitized Solar Cell. Sci. Rep. 7 (2017) 41470; doi: 10.1038/srep41470.

[8] H. Hug, M. Bader, P. Mair, T. Glatzel, T., Recent improvements in dye sensitized solar cells: A review. *Renew Sust Energ Rev* 52 (2015) 54-64.

[9] M. R. Narayan, Review: Dye sensitized solar cells based on natural photosensitizers. *Renew Sust Energ Rev* **16**, 208-215 (2012).

[10] D. Wei, Dye Sensitized Solar Cells. *Int. J. Mol. Sci.* 11 (2010) 1103-1113.

[11] M. K. Nazeeruddin, C. Klein, P. Liska, M. Grätzel, Synthesis of novel ruthenium sensitizers and their application in dye-sensitized solar cells. *Coord. Chem. Rev.* 249 (2005) 1460-1467.

[12] R. M. O'Donnell, P. G. Johansson, M. Abrahamsson, G. J. Meyer, Excited-State Relaxation of Ruthenium Polypyridyl Compounds Relevant to Dye-Sensitized Solar Cells. *Inorg. Chem.* 52, 6839-6848 (2013).

[13] S. M. Zakeeruddin *et al.*, Design, Synthesis, and Application of Amphiphilic Ruthenium Polypyridyl Photosensitizers in Solar Cells Based on Nanocrystalline TiO_2 Films. *Langmuir* 18 (2002) 952-954.

[14] R. Y. Ogura *et al.*, High-performance dye-sensitized solar cell with a multiple dye system. *Appl. Phys. Lett.* 94 (2009) 073308.

[15] C.-M. Lan *et al.*, Enhanced photovoltaic performance with co-sensitization of porphyrin and an organic dye in dye-sensitized solar cells. *Energy Environ Sci* 5 (2012) 6460-6464.

[16] A. Islam *et al.*, Enhanced Photovoltaic Performances of Dye-Sensitized Solar Cells by Co-Sensitization of Benzothiadiazole and Squaraine-Based Dyes. *ACS Appl. Mater. Interfaces* 8 (2016) 4616-4623.

[17] L. Han *et al.*, High-efficiency dye-sensitized solar cell with a novel co-adsorbent. *Energy Environ Sci* 5 (2012) 6057-6060.

[18] J.-H. Yum *et al.*, Efficient co-sensitization of nanocrystalline TiO_2 films by organic sensitizers. *J. Chem. Soc., Chem. Commun.* 44 (2007) 4680-4682

[19] Ehret, A.; L. Stuhl, L. and, and Spitler, M. T. Spectral Sensitization of TiO2 Nanocrystalline Electrodes with Aggregated Cyanine Dyes, The Journal of Physical Chemistry B 2001 105 (41), 9960-9965, DOI: 10.1021/jp011952

[20] T. Ono, T. Yamaguchi, and H. Arakawa, "Study on dye-sensitized solar cell using novel infrared dye," Solar Energy Materials and Solar Cells,, 2009, 93, 831-835

[21] Kensuke B. Takechi, P. K. Sudeep, Prashant V. Kamat, The Journal of Physical Chemistry B 2006 110 (33), 16169-16173, DOI: 10.1021/jp063651b

[22] C. I. Butoi,B. T. Langdon, and, and D. F. Kelley*, Electron-Transfer Dynamics in DTDCI/MoS2 and DTDCI/WS2 Nanoclusters, The Journal of Physical Chemistry B 1998 102 (48), 9635-9639 DOI: 10.1021/jp983008s

[23] Conceição, D.S.; Ferreira, D.P.; Ferreira, L.F.V. Photochemistry and Cytotoxicity Evaluation of Heptamethinecyanine Near Infrared (NIR) Dyes. Int. J. Mol. Sci. 2013, 14, 18557-18571.

[24] A. J. Winstead, *et al*. Microwave synthesis of cyanine dyes. *J. Microw Power Electromagn Energy* 44 (2010) 35-41.

[25] A. Winstead, & R. Williams, Application of Microwave Assisted Organic Synthesis to the Development of Near-IR Cyanine Dye Probes in *Environmental Biosensors* (ed. Somerset, V.) 237-254 (InTech, 2010).

[26] Lee, H.; Berezin, M. Y.; Henary, M.; Strekowski, L. & Achilefu, S. Fluorescence lifetime properties of near-infrared cyanine dyes in relation to their structures. *J. Photochem. Photobiol.* 200 (2008) 438-444.

[27] A. J. Winstead, Y. Williams R Fau - Zhang, C. Zhang Y Fau - McLean, S. McLean C Fau - Oyaghire, S. Oyaghire, Synthesis of Quaternary Heterocyclic Salts. *Molecules* 18 (2013) 14306–14319.

[28] X. Fei, Y. Gu, Progress in modifications and applications of fluorescent dye probe. *Prog. Nat. Sci.Mater* 19 (2009) 1-7.

[29] J. O. Escobedo, O. Rusin, S. Lim, R. M. Strongin R. M. NIR Dyes for Bioimaging Applications. *Curr Opin Chem Biol* 14 (2010) 64.

[30] W. Sun, S. Guo, C. Hu, J. Fan, X. Peng, Recent Development of Chemosensors Based on Cyanine Platforms. *Chem. Rev.* 116 (2016) 7768-7817.

[31] X. Ma et al., A high-efficiency cyanine dye for dye-sensitized solar cells. *Tetrahedron* 64 (2008) 345-350.

[32] K. Funabiki et al., Design of NIR-Absorbing Simple Asymmetric Squaraine Dyes Carrying Indoline Moieties for Use in Dye-Sensitized Solar Cells with Pt-Free Electrodes. *Org. Lett.* 14 (2012) 1246-1249.

[33] W. Wu, F. Guo, J. Li, J. He, J. Hua, J. New fluoranthene-based cyanine dye for dye-sensitized solar cells. *Synth. Met.*160 (2010) 1008-1014

[34] W. Ghann, *et a*l. Interaction of Sensitizing Dyes with Nanostructured TiO_2 Film in Dye-Sensitized Solar Cells Using Terahertz Spectroscopy. Sci. Rep. **6** (2016) 30140

[35] L. Amadi *et al*. Creation of Natural Dye Sensitized Solar Cell by Using Nanostructured Titanium Oxide. Nanosci. Nanoeng. 3 (2015) 25-35.

[36] S. Yadav, *et al*. Natural Light-harvesting Sensitizers for Dye Sensitized Solar Cell. Energ. Environ. Eng. 3 (2015) 94 - 99.

[37] L. Zhang, J. M. Cole, Anchoring Groups for Dye-Sensitized Solar Cells. *ACS ACS Appl. Mater. Interfaces* 7 (2015) 3427-3455.

[38] M. Pastore, F. D. Angelis, First-Principles Computational Modeling of Fluorescence Resonance Energy Transfer in Co-Sensitized Dye Solar Cells. *J. Phys. Chem. Lett.* 3 (2012) 2146-2153.

[39] L. Li et al.,, A simple modification of near-infrared photon-to-electron response with fluorescence resonance energy transfer for dye-sensitized solar cells. *J. Power Sources* 264 (2014) 254-261.

[40] S. E. Koops, B. C. O'Regan, P. R. F. Barnes, J. R. Durrant, Parameters Influencing the Efficiency of Electron Injection in Dye-Sensitized Solar Cells. *J. Am. Chem. Soc* 131 (2009) 4808-4818.

[41] P. M. Kumar, S. Badrinarayanan, M. Sastry Nanocrystalline TiO_2 studied by optical, FTIR and X-ray photoelectron spectroscopy: correlation to presence of surface states. *Thin Solid Films* 358 (2000) 122-130

[42] J.-Y. Zhang et al., Nanocrystalline TiO_2 films studied by optical, XRD and FTIR spectroscopy. *J. Non-Cryst. Solids* 303 (2002) 134-138

[43] Z. Shen et al. Synthesis and Photovoltaic Properties of Powerful Electron-Donating Indeno[1, 2-b]thiophene-Based Green D–A–π–A Sensitizers for Dye-Sensitized Solar Cells. *ACS Sustain. Chem. Eng.* 4 (2016) 3518-3525.

[44] M. S. Góes et al., Impedance Spectroscopy Analysis of the Effect of TiO_2 Blocking Layers on the Efficiency of Dye Sensitized Solar Cells. *J. Phys. Chem. C*116 (2012) 12415-12421.

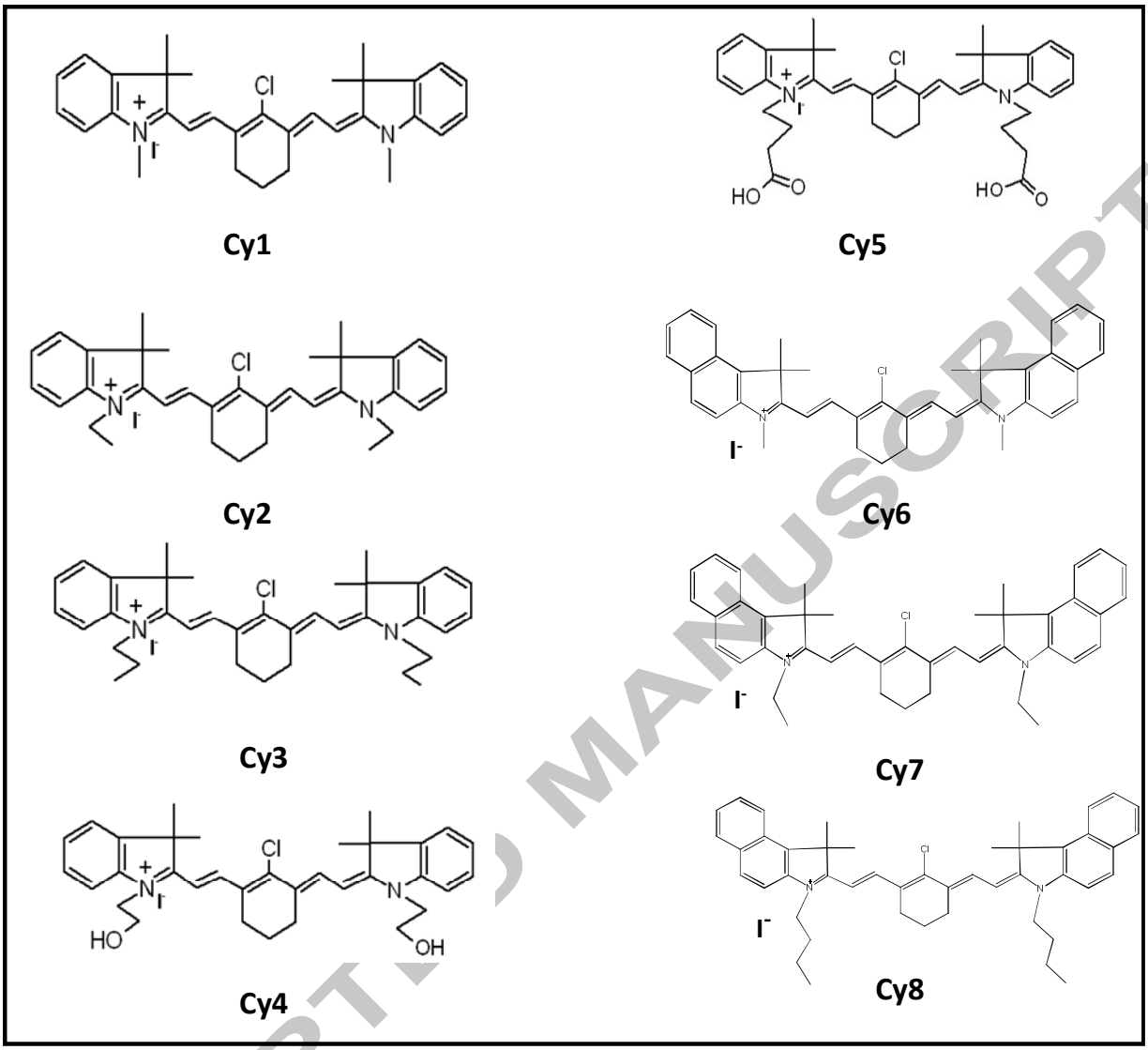

Figure 1: Structures of the eight cyanine dyes investigated: Cyanine 1 (Cy1); Cyanine 2 (Cy2);Cyanine (Cy3); Cyanine 4 (Cy4); Cyanine 5 (Cy5); Cyanine 6 (Cy6); Cyanine 7 (Cy7); Cyanine 8 (Cy8)

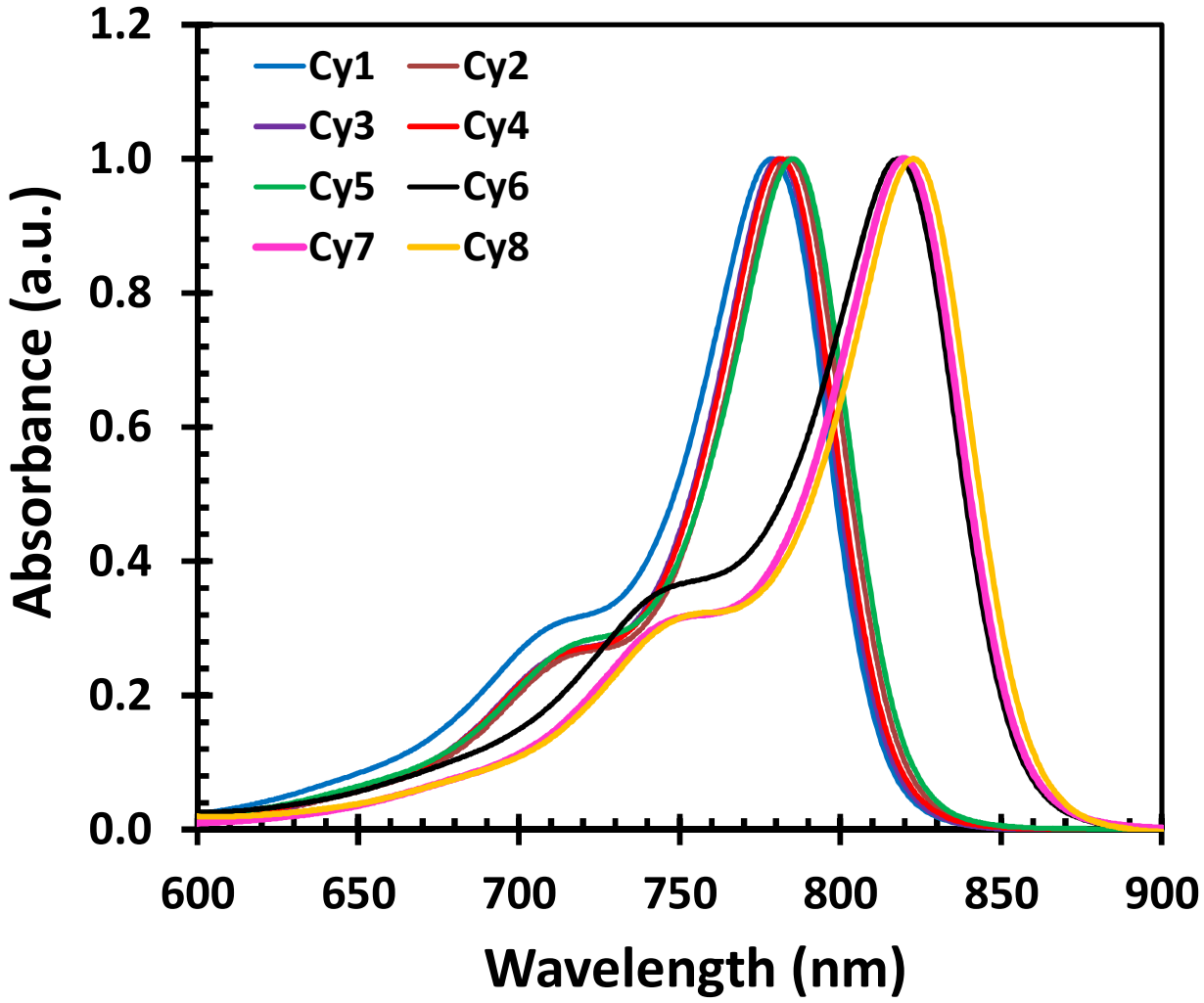

Figure 2: Absorption spectra of eight cyanine dyes measured in ethanol (10 µM) showing differences in absorption between Cy1 – Cy5 and Cy6 – Cy8

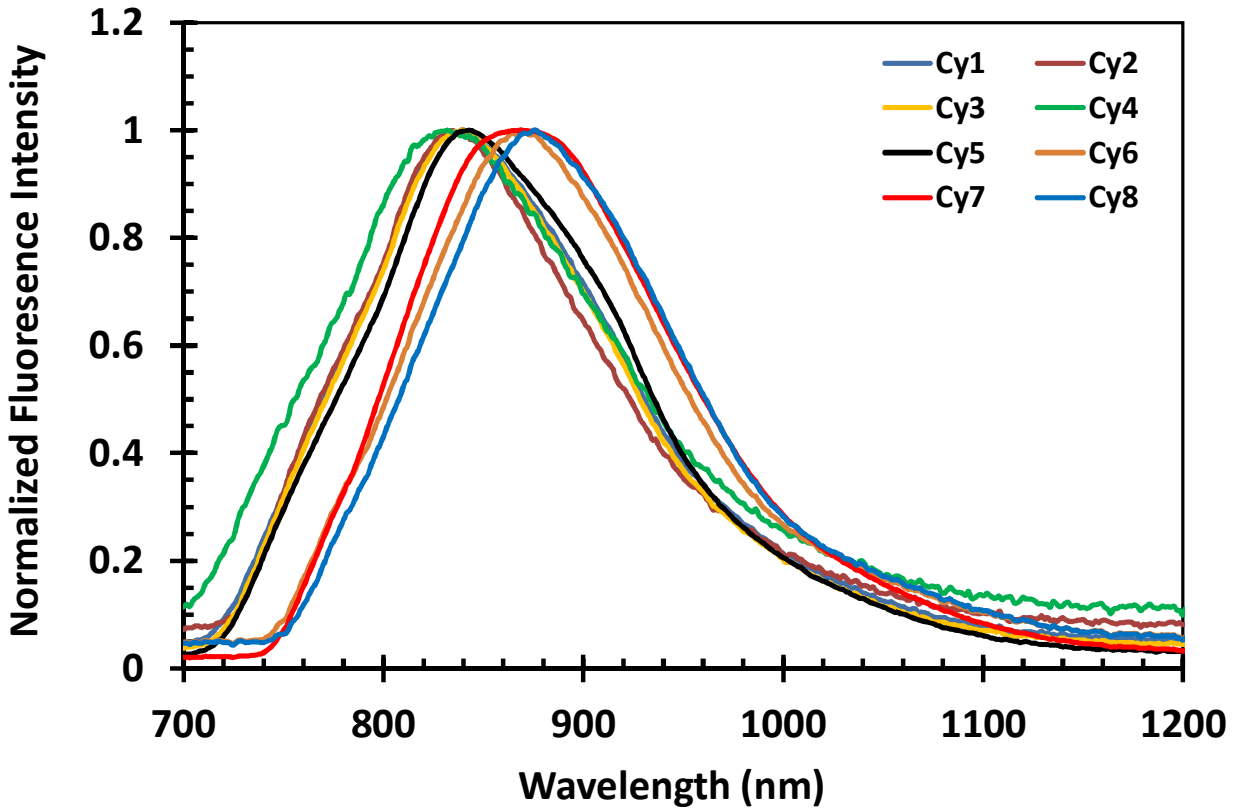

Figure 3: Emission spectra of eight cyanine dyes measured in ethanol showing differences in absorption between Cy1 – Cy5 and Cy6 – Cy8. Wavelength of excitation is 700 nm.

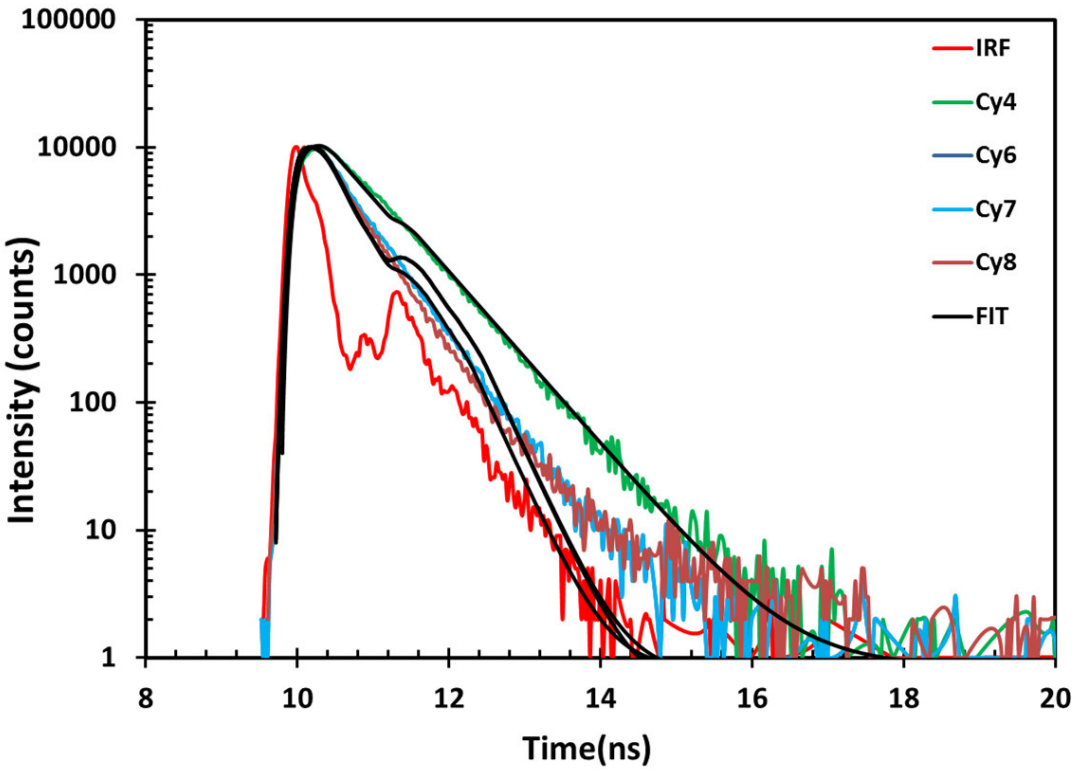

Figure 4: Fluorescence Lifetime Measurement of selected cyanine dyes: Cy4, Cy6, Cy7 &Cy8 and the instrument response function. Blue curve: Instrument response function; black curve: fit for various fluorescence decays.

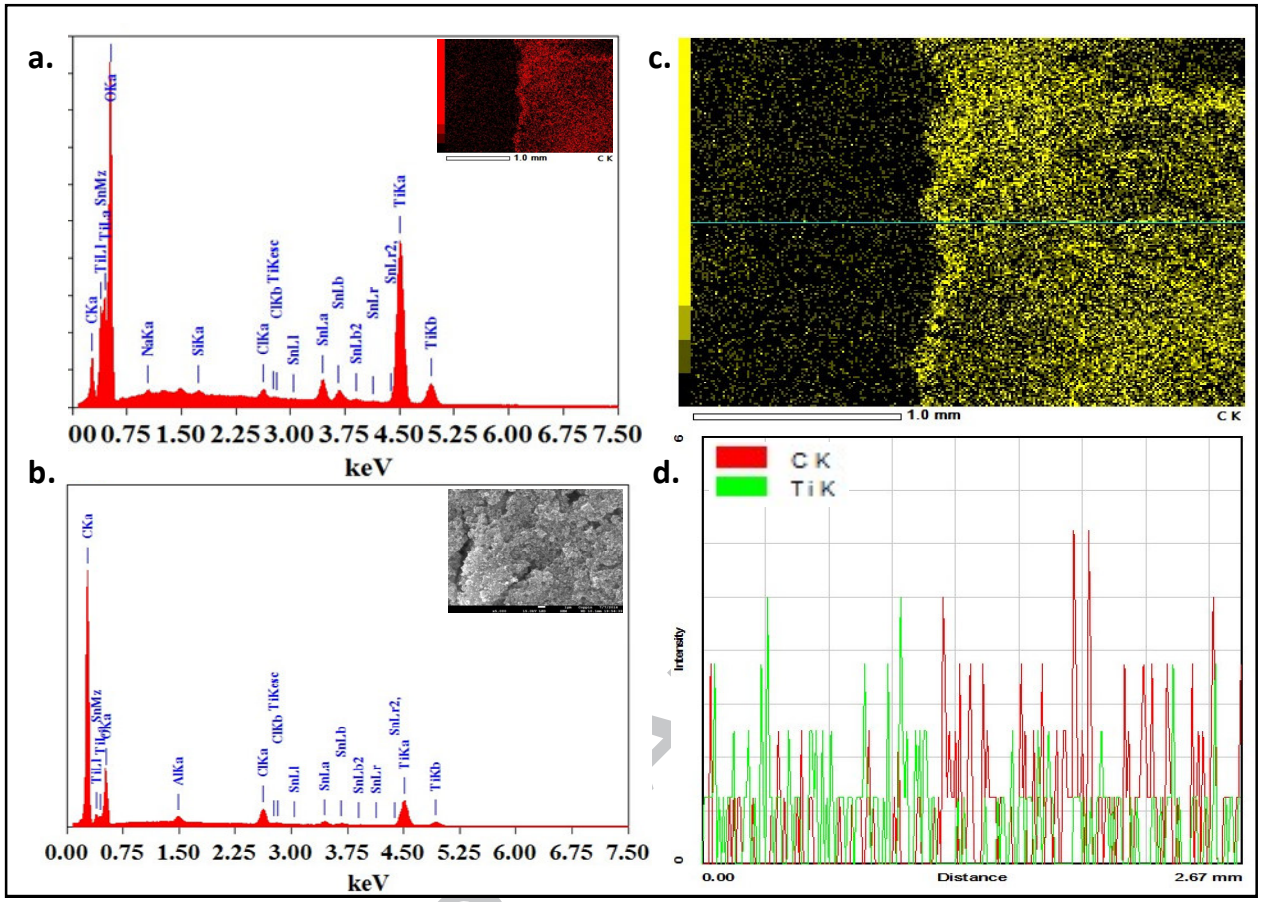

Figure 5: SEM and EDS Analysis: (a) EDS of bare TiO_2 coated FTO glass; (inset) TiO_2 film partially covered with cyanine dye (b) EDS of cyanine dye sensitized TiO_2 /FTO glass; (inset) Cyanine dye sensitized TiO_2 /FTO glass (c) Partially dyed TiO_2 film/FTO glass for line profile analysis ;(d) Line profile analysis of partially dyed TiO_2 /FTO; insets for (a) and (b) corresponding to SEM images used for EDS analysis

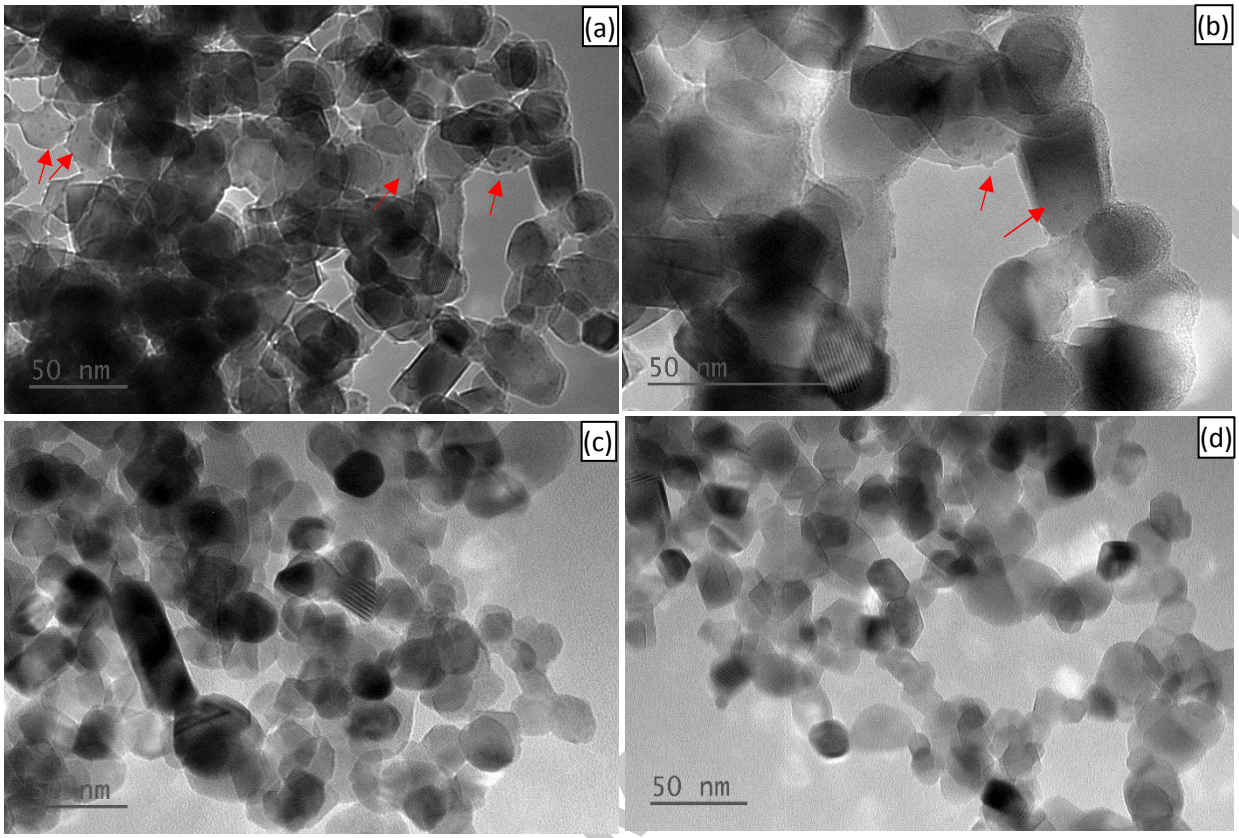

Figure 6: High-resolution TEM images of the cyanine dye/TiO_2 and the TiO_2 nanoparticles: (a) (b) high resolution TEM images of Cyanine dye/TiO_2, and (c) (d) of TiO_2 nanoparticles without dye

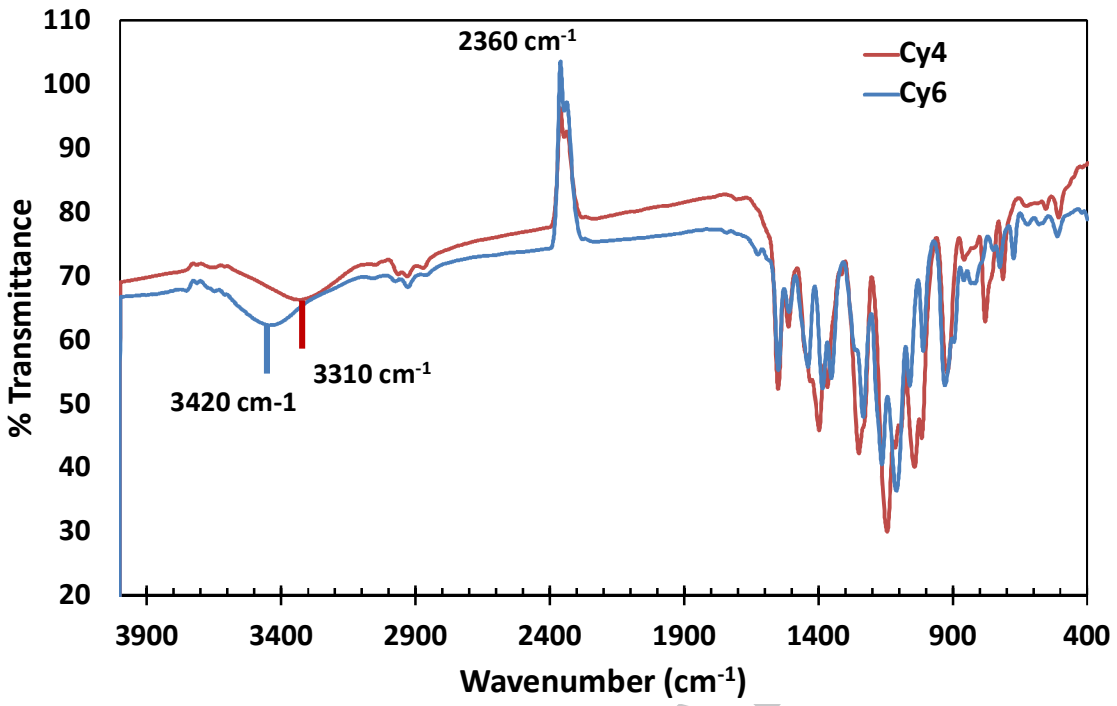

Figure 7: FT-IR spectrum of Cy4 (red) and Cy6 (blue) showing variation in wavelength of peak transmittance between the two different cyanine dye-sensitized TiO_2 representing the two categories of dyes investigated.

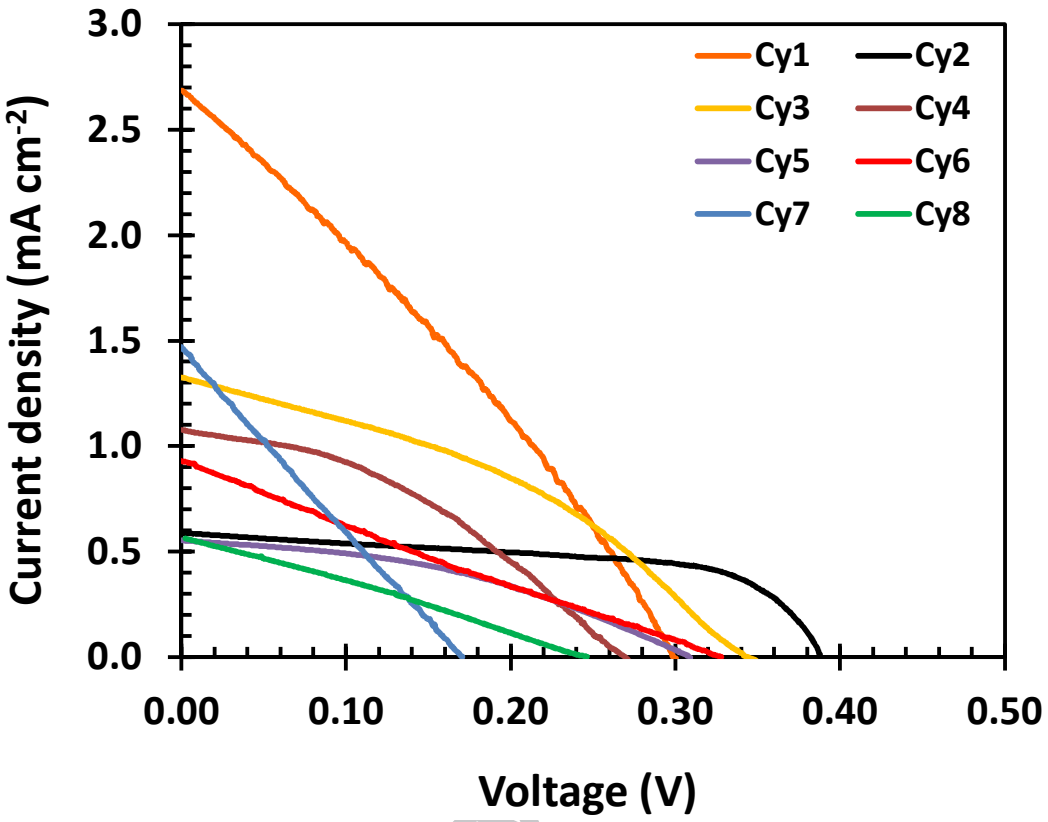

Figure 8: Photocurrent-voltage characteristics for cyanine dye sensitized solar cell measured under illumination of 100mW/cm^2 (1.5 AM)

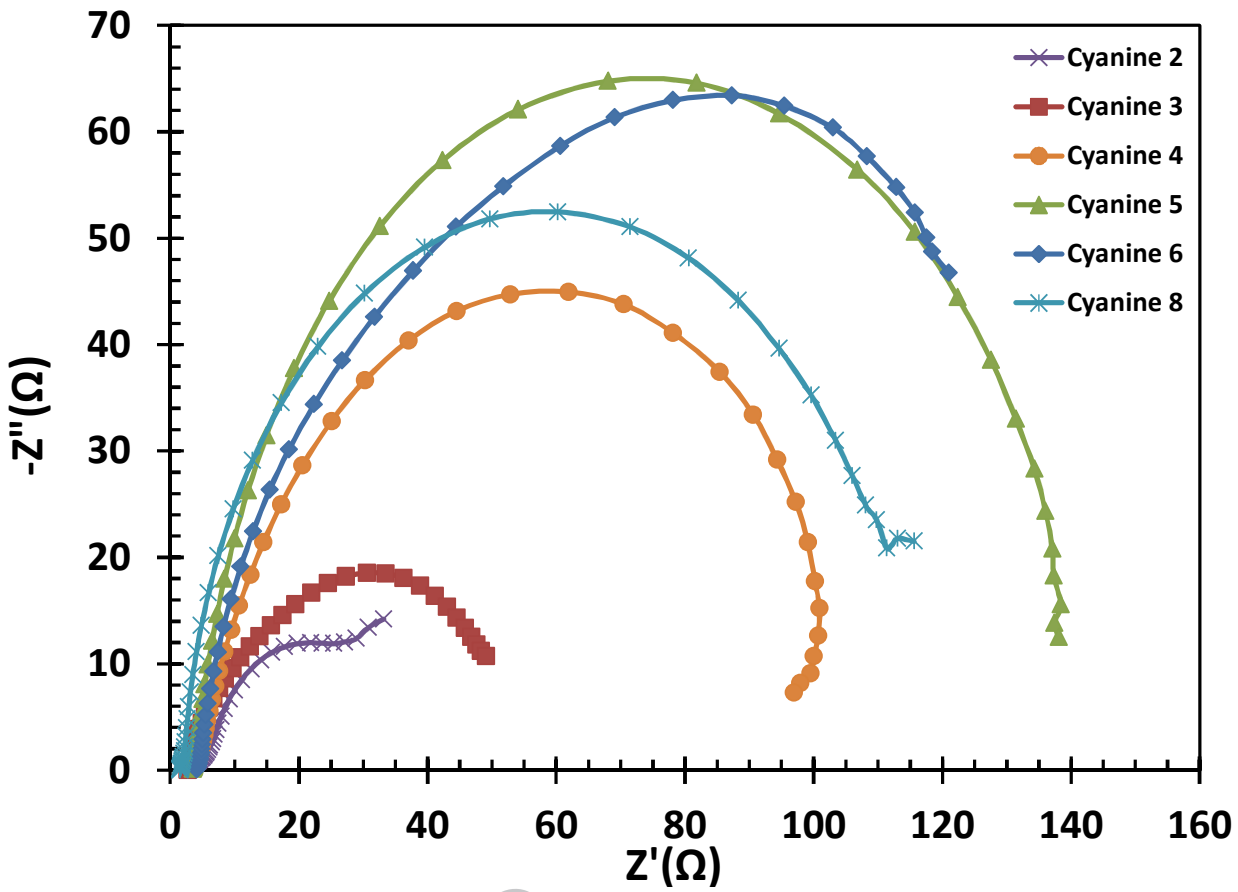

Figure 9: Nyquist plots for the fabricated Cyanine dye Sensitized Solar Cells showing differences in the resistances to charge transfer.

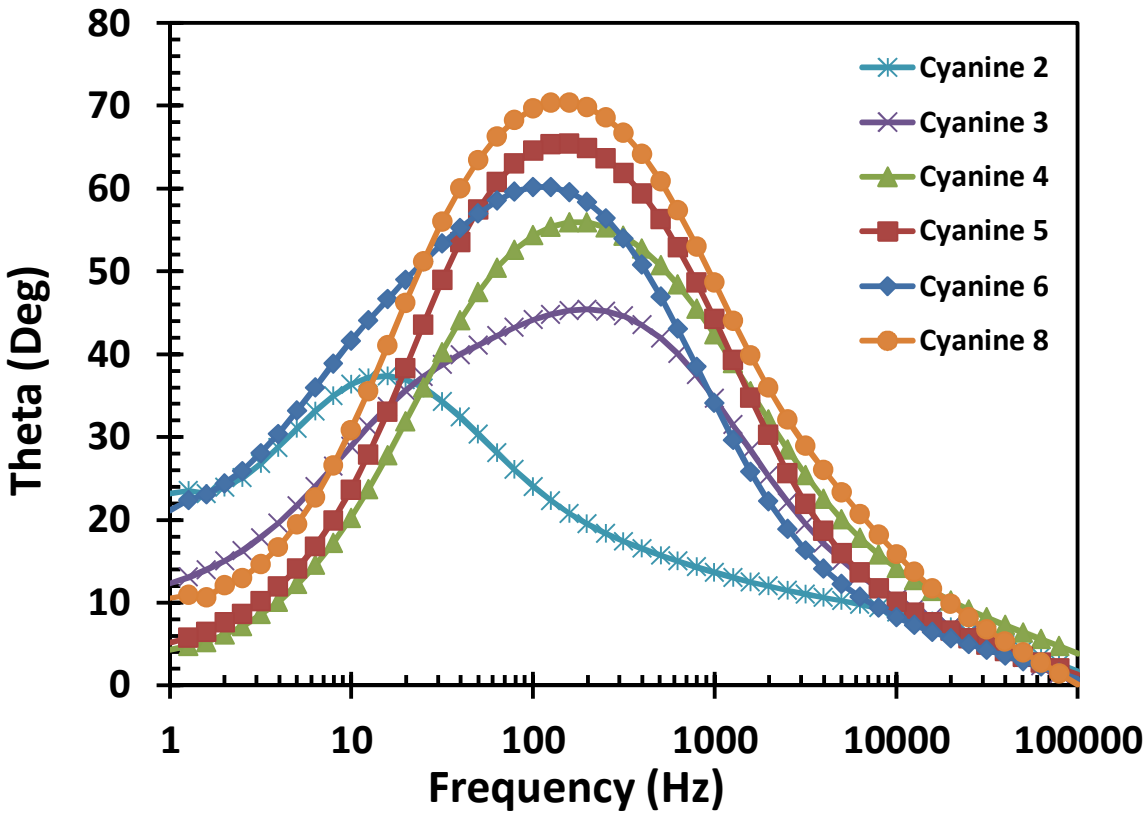

Figure 10: Bode plots for the fabricated Cyanine dye Sensitized Solar Cells

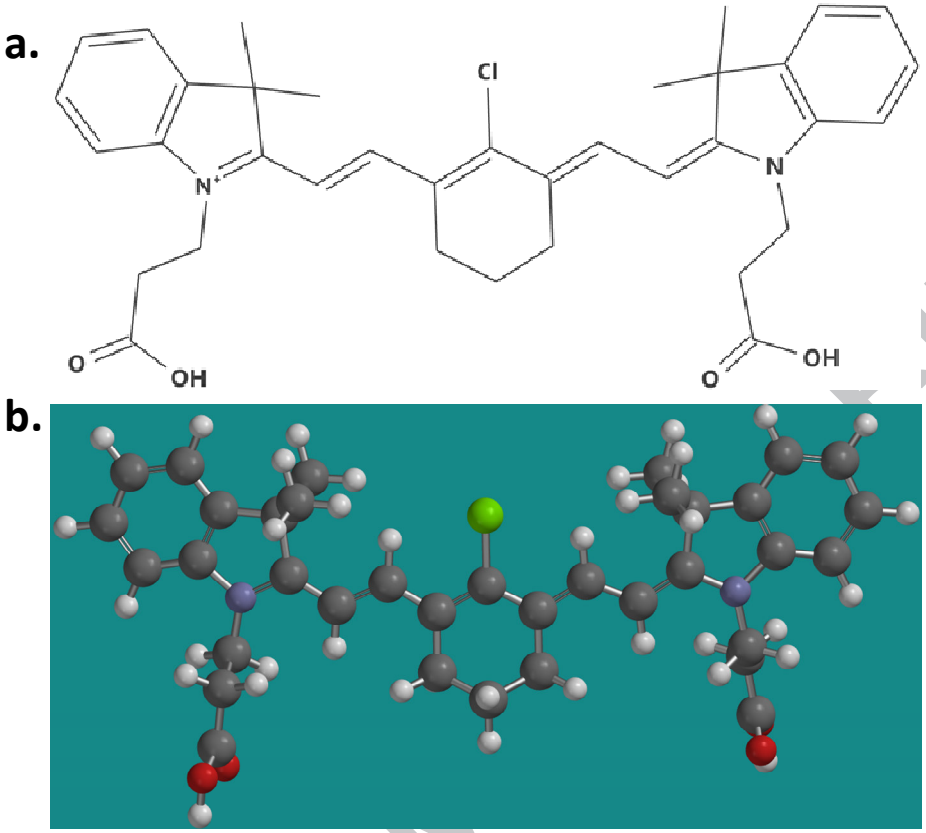

Figure 11: Lewis structure (a) and 3d structure (b) of Cy5.

a.

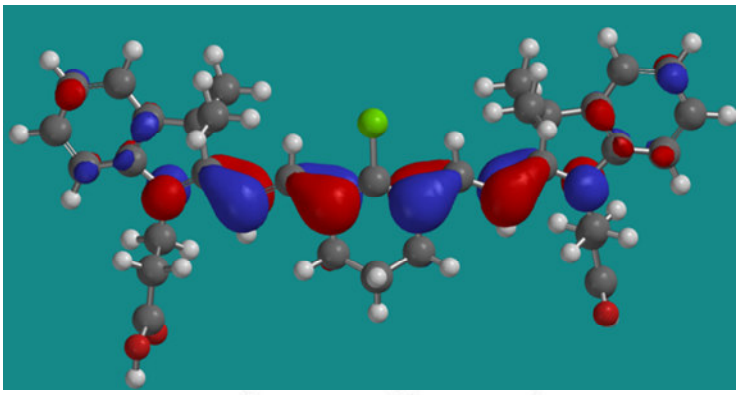

LUMO surface and orbital energy diagram

E_LUMO -3.95 eV

b.

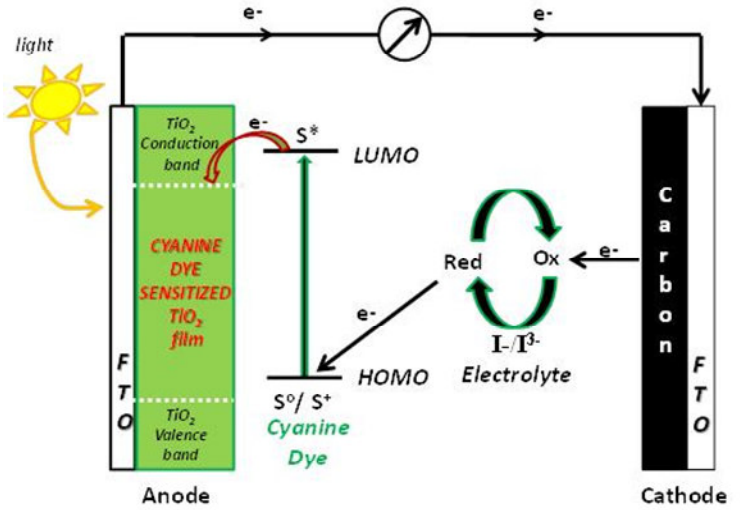

Band Gap E_LUMO – E_HOMO = 4.91 eV

c.

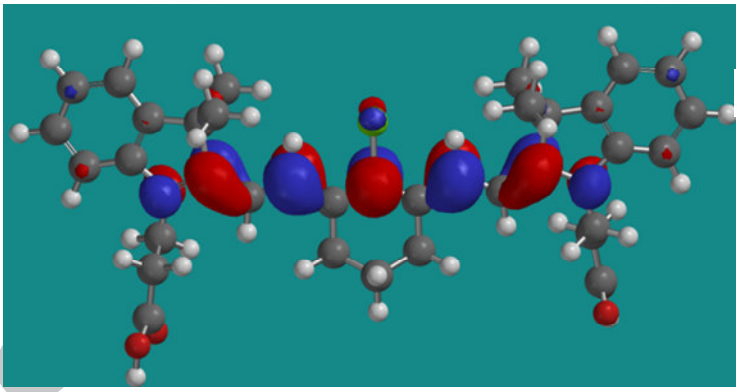

HOMO surface and orbital energy diagram

E_HOMO -8.86 eV

Figure 12: (a) LUMO surface and orbital energy diagram for Cy5 (b) Operation principles of DSSC with Cy5 and (c) HOMO surface and orbital energy diagram for Cy5

Table 1: Photophysical Properties of Cyanine Dyes

Dye	Absorption λabs(nm)	Emission λems (nm)	Stokes shift (nm)	Quantum Yield	Detection Sensitivity (M)	Molar Absorptivity L mol^{-1} cm^{-1}	MW (g/mol)
Cy1	779	840	61	0.16 ±0.0002	1E-08	2.8E+05	611.00
Cy2	781	838	57	0.22 ±0.0059	7.2E-09	1.6E+05	639.05
Cy3	781	840	59	0.20 ±0.0015	1.7E-08	1.2E+05	667.10
Cy4	782	832	50	0.19 ±0.0254	4E-09	4.3E+05	671.03
Cy5	785	843	58	0.16 ±0.0229	1.8E-08	2.4E+05	727.03
Cy6	818	869	51	0.18 ±0.0225	7.5E-08	2.1E+05	711.12
Cy7	820	869	49	0.19 ±0.0259	8.2E-08	1.9E+05	739.17
Cy8	823	876	53	0.14 ±0.0320	9.1E-08	1.7E+05	795.28

Table 2: Fluorescence Lifetime Measurement of Cyanine Dyes

Sample Name	Lifetime (ns)	
	?$_f$	±
Cy1	0.18	0.00187
Cy2	0.68	0.0032
Cy3	0.46	0.0059
Cy4	0.48	0.0058
Cy5	0.48	0.0061
Cy6	0.34	0.0027
Cy7	0.43	0.0024
Cy8	0.32	0.0021

Table 3: Current Voltage Characteristics of Cyanine dye Sensitized Solar Cells

DYE	Isc (mA/cm^2)	Voc (V)	Imp (mA/cm^2)	Vmp (V)	Fill Factor (ff)	Efficiency (%)	STDEV ±
Cyanine 1	2.69	0.30	1.51	0.16	0.30	0.24	0.07
Cyanine	0.59	0.39	0.43	0.32	0.60	0.13	0.06

2							
Cyanine 3	1.33	0.35	0.82	0.21	0.37	0.17	0.02
Cyanine 4	1.08	0.27	0.70	0.16	0.38	0.11	0.05
Cyanine 5	0.55	0.31	0.37	0.18	0.39	0.07	0.006
Cyanine 6	0.93	0.33	0.38	0.19	0.24	0.07	0.027
Cyanine 7	1.47	0.17	0.71	0.09	0.26	0.06	0.026
Cyanine 8	0.62	0.25	0.30	0.13	0.25	0.04	0.02

Research Highlights:

The photophysical properties of eight heptametine cyanine dyes were investigated with respect to their structure.

Morphological studies carried out with TEM and SEM demonstrated a good interaction between titanium dioxide nanoparticles and cyanine dyes.

The performance of cyanine dye sensitized solar cell is influenced by the structure of the cyanine dye.

Graphical Abstract:

Eight heptamethine cyanine dyes were synthesized and investigated for application in dye sensitized solar cell. The photophysical properties of the dyes revealed differences in optical properties with respect to their structure. The performance of the cyanine dye-sensitized solar cells conformed to the photophysical properties of the cyanine dyes.